Coherent Control of Collective Spontaneous Emission through Self-Interference

Lei Qiao[1,*] and Jiangbin Gong[1,2,†]
[1]Department of Physics, National University of Singapore, Singapore 117551, Singapore
[2]Center for Quantum Technologies, National University of Singapore, Singapore 117543, Singapore

(Received 13 April 2022; accepted 1 August 2022; published 24 August 2022)

As one of the central topics in quantum optics, collective spontaneous emission such as superradiance has been realized in a variety of systems. This Letter proposes an innovative scheme to coherently control collective emission rates via a self-interference mechanism in a nonlinear waveguide setting. The self-interference is made possible by photon backward scattering incurred by quantum scatterers in a waveguide working as quantum switches. Whether the interference is constructive or destructive is found to depend strongly on the distance between the scatterers and the emitters. The interference between two propagation pathways of the same photon leads to controllable superradiance and subradiance, with their collective decay rates much enhanced or suppressed (also leading to hyperradiance or population trapping). Furthermore, the self-interference mechanism is manifested by an abrupt change in the emission rates in real time. An experimental setup based on superconducting transmission line resonators and transmon qubits is further proposed to realize controllable collective emission rates.

DOI: 10.1103/PhysRevLett.129.093602

Introduction.—Waveguide quantum electrodynamics has recently been a growing area in quantum optics with important applications in quantum information processing [1–5]. Different integrations of quantum emitters (QEs) with nanophotonic structures have been achieved, such as guided surface plasmons confined on a conducting nanowire with individual optical emitters [6,7], photonic nanowire coupled by embedded quantum dots [8,9], or superconducting transmission line with superconducting qubits [10–12]. These physical platforms make it possible to let QEs interact with one-dimensional bosonic modes with nontrivial dispersions [13–27]. Advances in designing and probing light-matter interactions have also stimulated the investigation of collective phenomena such as superradiance and subradiance [28–36], cavity antiresonance spectroscopy [37], and nonequilibrium collective phase transition [38,39].

As a typical collective emission, Dicke superradiance has been demonstrated in systems of hot atoms [40,41], cold atoms [42,43], trapped ions [44–46], superconducting qubits [47,48], etc. Its counterpart with reduced emission rate is termed subradiance. Transitions between superradiant and subradiant states have been realized in superconducting circuits by initially applying a phase gate on each qubit [49]. Superradiance and subradiance are highly relevant to quantum memory in connection with the writing and reading of quantum information [50,51]. However, to date continuously controllable collective emission rate without using external driving fields [52–54] remains a challenge for almost all QE systems.

In this Letter we reveal an unknown aspect of spontaneous emission in a nonlinear waveguide setting. We consider quantum scatterers in addition to general quantum emitters in the same waveguide. The emitted photon propagating in the waveguide can be bounced back by the scatterers. The backward scattered photon then interferes with the other branch of the photon propagating in the opposite direction. Such self-interference is exploited to achieve continuous and extensive control of the spontaneous emission rate of QEs. Indeed, even the transition from superradiance to subradiance can be readily achieved if we control certain features of the quantum scatterers, such as its resonance frequency and the QE-scatterer distance. Specifically, the QE-scatterer distance is found to be a crucial parameter to induce constructive or destructive interference. An experimental setup based on superconducting transmission line resonators and transmon qubits is further proposed to realize continuously controllable collective emission rates.

Model.—Consider a system consisting of a one-dimensional array of tunneling-coupled cavities which accommodate one assembly of QEs at position $x = x_1$ and a second collection of two-level atoms at x_2, respectively. A schematic plot of this configuration is shown in Fig. 1. Atoms at x_2 play the role of quantum scatterers, through which the spontaneous emission dynamics of QEs at x_1 is to be manipulated. Though playing two different roles, these two collections of atoms will be treated with similar notation, indexed by A and B, respectively, and assumed to have excited states $|e^A\rangle$, $|e^B\rangle$ and ground states $|g^A\rangle$, $|g^B\rangle$, separated in energy by frequencies Ω_A and Ω_B (we set $\hbar = 1$ throughout). The tunneling-coupled photonic waveguide forms a lattice, modeled by the following tight-binding Hamiltonian:

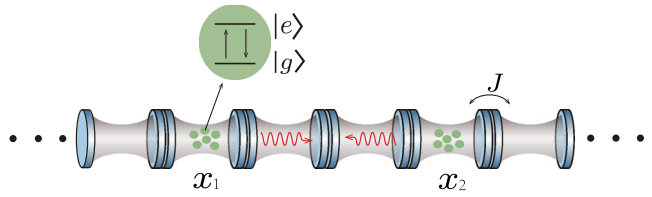

FIG. 1. Schematic of a waveguide setup. A one-dimensional array of resonators with nearest-neighbor tunneling J hosts an assembly of quantum emitters at x_1 and a second collection of two-level atoms as quantum scatterers at x_2.

$$H_{\rm ph} = \sum_x \omega_c a_x^\dagger a_x + J\sum_x (a_{x+1}^\dagger a_x + a_x^\dagger a_{x+1}), \quad (1)$$

where $a_x^\dagger$ is the creation operator of the waveguide mode at position x, and ω_c is the resonance frequency of a single cavity. For convenience, we assume the lattice constant to be $a = 1$ throughout. The total Hamiltonian describing the system is then

$$H = H_{\rm ph} + \sum_j \Omega_{j,A}|e_j^A\rangle\langle e_j^A| + \sum_j \Omega_{j,B}|e_j^B\rangle\langle e_j^B| + \sum_j (V_{j,A}\sigma_{j,A}^+ a_{x_1} + V_{j,B}\sigma_{j,B}^+ a_{x_2} + \text{H.c.}), \quad (2)$$

where $\sigma_{j,A}^+$ and $\sigma_{j,B}^+$ are the creation operators for the jth atom in each assembly and $V_{j,A}$ and $V_{j,B}$ are the respective coupling strengths. For the case of only one QE with weak coupling ($V \ll J$), the QE decays with the radiation rate $\Gamma = V^2/J$ if the emitter is near resonance with the frequency of a single cavity [55]. In the single excitation subspace, the spectrum of Eq. (2) comprises discrete localized bound states and a continuum of delocalized dressed states with energy $\omega_k = \omega_c + 2J\cos(k)$ versus the mode wave vector k, thus forming a scattering band with ω_c being the band central frequency with bandwidth $4J$ ($J > 0$). The said bound states result in the known fractional trapping of an emitted photon and nonexponential dynamics of the spontaneous emission [56,57]. Note also that the peak photon group velocity is $v_g^m = 2J$ reached by the wave vector $k_m = \pm\pi/2$.

General theoretical considerations.—Let us now assume that the QEs and the quantum scatterers are separated by a distance $\Delta x \equiv |x_2 - x_1|$, which is less than half of the coherence length $\sim v_g^m/\Gamma$ of a spontaneously emitted photon. The initial state of the whole system is that one of the QEs is excited, or two of the QEs are in the superpositions of their excited states, with the photon field in vacuum. This hence places the whole wave function in the single-excitation invariant subspace. The time-evolving state at time t can be written as

$$|\psi(t)\rangle = \left\{\sum_i \sum_{j=1}^{M_i} C_j^i(t)\sigma_{j,i}^+ + \sum_k C_k(t)a_k^\dagger\right\}|g, \text{vac}\rangle, \quad (3)$$

where $i = A$, B, and $a_k^\dagger = (1/\sqrt{N})\sum_x e^{ikx}a_x^\dagger$. M_i is the number of the QEs or of the scatterers. C_j^i is the excitation amplitude for the jth atom in each collection of atoms, C_k is the amplitude of the waveguide mode with momentum k. Without loss of generality, we assume that only QEs with indices j_n may be excited at time zero, i.e., $C_{j_n}^A(0) \neq 0$, $C_j^A(0) = 0$ ($j \neq j_n$), and $C_j^B(0) = C_k(0) = 0$. If initially at most two excited QEs indexed by j_1 and j_2 are involved in the initial excitation, then exact results about their ensuing time dependence can be obtained [58]:

$$C_{j_1}^A(t) = \frac{L_1(s)C_{j_1}^A(0) + L_2(s)C_{j_2}^A(0)}{G(s)}e^{st}|_{s=-i\Omega_A} + \sum_m \frac{iL_2(s)[C_{j_1}^A(0) + C_{j_2}^A(0)]}{(is - \Omega_A)[G(s)]'}e^{st}|_{s=x_m} - \sum_{\alpha=\pm}\int_{-1}^{1}\frac{[Q_1^\alpha C_{j_1}^A(0) + Q_2^\alpha C_{j_2}^A(0)]e^{i2Jyt}}{2\pi i\alpha(y + \Omega_A)[Q_1^\alpha - Q_2^\alpha]}dy, \quad (4)$$

where $L_{1,2}(s)$ and $G(s)$ strongly depend on the separation parameter Δx, $Q_{1,2}^\pm$ are explicit functions of the integration variable y, and x_m is the roots of the equation $G(s) = 0$ [58]. The imaginary part of each x_m corresponds to the inverse of the system's eigenenergies of the localized photon-QE dressed states. In fact, the second term on the right-hand side of Eq. (4) originates from the system's photon-QE bound states with nonzero field amplitudes. $C_{j_2}^A(t)$ can be obtained by exchanging the positions of $C_{j_1}^A(0)$ and $C_{j_2}^A(0)$ in Eq. (4). In obtaining the analytical expressions above, it has been assumed that each collection of atoms (namely, among the QEs, or among the scatterers) is identical and thus $\Omega_{j,i}$ and $V_{j,i}$ are independent of the atom index j, denoted by Ω_A, Ω_B, V_A, and V_B.

Cases with one single emitter.—To gain some important insights first, we consider a single QE indexed by j_1 coupled with multiple scatterers through the waveguide, with the initial state $|\psi(0)\rangle = \sigma_A^+|g, \text{vac}\rangle$. The time evolution of the excited state population $P_e(t) = |C_{j_1}^A(t)|^2$ is shown in Fig. 2(a) versus the detuning parameter $\Delta_B = \Omega_B - \omega_c$ depicting the scatterers, with the QE-scatterer separation $\Delta x = 7$ (i.e., 7 lattice constants) as an example. At early times, the emission dynamics matches well with that of a normal decay process $P_e(t) \approx e^{-\Gamma_1 t}$ with $\Gamma_1 = V_A^2/J$ (assuming $V_A \ll J$), without feeling the presence of the scatterers. Later the scatterers make a dramatic difference during the spontaneous emission process. In particular, as the main reason to introduce the scatterers in the first place, the scatterers as two-level systems can extensively control the coherent transport of a single photon in the waveguide, including a complete reflection of the emitted photon [5]. Hence, once part or even the whole of the propagating photon toward the scatterers comes back to the decaying QE, it will interfere with the other branch of

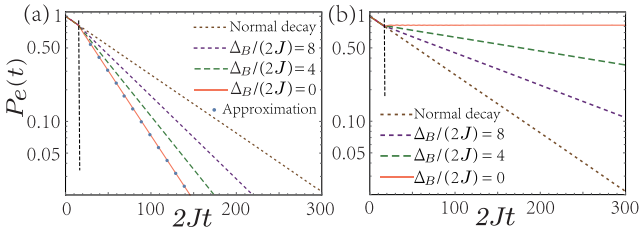

FIG. 2. (a) Excited state population $P_e(t)$ versus detuning Δ_B for $\Delta x = 7$. (b) Excited state population $P_e(t)$ versus detuning Δ_B for $\Delta x = 8$. The parameters are $V_A/(2J) = 0.08$, $V_B/(2J) = 1.8$, and $\Delta_A/(2J) = 0$, the number of emitters is $M_A = 1$ and that of scatterers is $M_B = 2$. In both (a) and (b) the vertical dashed lines indicate the time of arrival of a reflected photon.

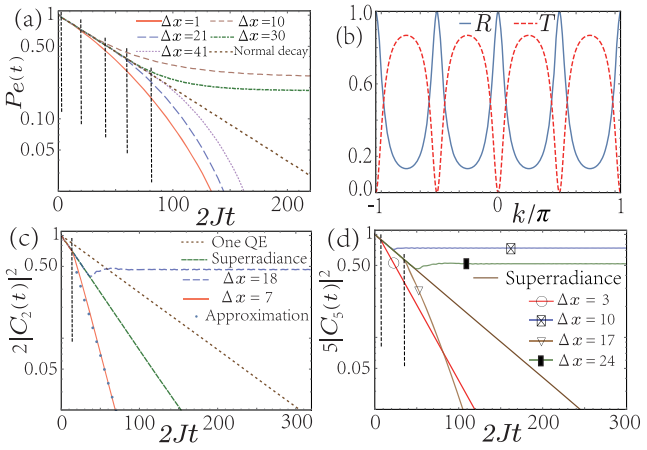

FIG. 3. (a) Excited state population $P_e(t)$ versus Δx, with $V_A/(2J) = 0.09$, $V_B/(2J) = 0.07$, $\Delta_A/(2J) = 0$, $\Delta_B/(2J) = 0$, $M_A = 1$, and $M_B = 2$. (b) Reflection coefficient $R = |r_k|^2$ and transmission coefficient $T = |1 + r_k|^2$ as a function of momentum k. Parameters are $\Delta_B/(\sqrt{M_B}V_B) = 0$, $J/(\sqrt{M_B}V_B) = 1.13$. (c) Excited state population $2|C_2(t)|^2$, with $\Delta_A/(2J) = 0$, $\Delta_B/(2J) = 0$, $V_A/(2J) = 0.08$, $V_B/(2J) = 1.27$, $M_A = 2$, and $M_B = 2$. (d) Excited state population $5|C_5(t)|^2$, with $\Delta_A/(2J) = 0$, $\Delta_B/(2J) = 0$, $V_A/(2J) = 0.04$, $V_B/(2J) = 1.0$, $M_A = 5$, and $M_B = 2$. Different vertical dashed lines indicate the different times of arrival of a reflected photon.

the photon propagating along the other direction. Supporting this physical picture, Fig. 2(a) depicts an abrupt change of the radiation rate once t reaches $t_0 \approx 2\Delta x/(2J)$, yielding a cascade of stimulated emission. In terms of the real-time dynamics, we are witnessing an intriguing scenario that an emitted photon, when being bounced back, can further boost the emission process that has not been completed yet. The degree of enhancement is continuously controlled by the frequency of the scatterers, as evidenced by the shown strong dependence of the emission rates versus the detuning parameter Δ_B.

Continuing our investigations of the cases with $\Delta x = 2n + 1$ (n being an integer), let us further assume that the quantum scatterers are near resonance with each single cavity with small Δx, plus the conditions $V_A \ll 2J$ and $\sqrt{M_B}V_B \sim 2J$. The enhanced emission rate under these conditions is found to be $P_e(t) \approx [M_B V_B^2/(4J^2) - \alpha_1/2]^2 e^{-2J\alpha_1 t}/\beta_1$ with $\alpha_1 = V_A^2/(J^2 - \Delta x V_A^2/2)$ and β_1 is a time-independent quantity [58]. As can be seen in Fig. 2(a), our approximate theoretical results agree well with the exact results obtained from Eq. (4). For Δx being small enough, the radiance rate is 2 times the normal decay rate. Although there is only one QE here, the emission rate is much enhanced and even beyond two-QE Dicke superradiance. The physical understanding is the following: The QE interferes with itself via a delayed photon; thus it can effectively realize collective interference and hence achieve superradiance.

Next we consider cases with $\Delta x = 2n$. A few computational examples with $\Delta x = 8$ are shown in Fig. 2(b), where suppressed emission rates are clearly observed. As the frequency of the scatterers is tuned from ω_c to the values far away from the photon band, the suppression becomes weak and ultimately the emission comes back to the normal decay. It is curious to qualitatively understand why superradiance and subradiance are observed for $\Delta = 2n + 1$ and $\Delta = 2n$ in Figs. 2(a) and 2(b), respectively. If $\Delta x = 2n + 1$, the phase difference incurred by the round travel of the bounced photon can be estimated as $|k_m|(2\Delta x) = (2n + 1)\pi$, if considering the main wave component around $k_m = \pm\pi/2$ with the largest group velocity. Also accounting for the π shift associated with a complete photon reflection, the overall phase difference between the bounced photon and the original photon is thus $2n\pi$, yielding constructive interference and hence enhanced emission. By contrast, if $\Delta x = 2n$ is chosen, then the overall phase difference between the two interfering pathways is $(2n + 1)\pi$, thus producing destructive interference and leading to suppression of the emission and thus subradiance. Confirming this understanding, in Fig. 3(a), we further show how the emission rates for weak coupling V_B are changed over a wide range if the QE-scatterer distance Δx is adjusted.

Our results above have clearly indicated the important role of the backward scattering in the self-interference mechanism. It is hence useful to examine some details of the scattering process. When the radiation field reaches the scatterers, part of the field is reflected with the reflection amplitude r_k given by $r_k = M_B V_B^2[i2J|\sin(k)|(\omega_k - \Omega_B) - M_B V_B^2]^{-1}$ [58]. The effect of M_B scatterers is equivalent to that of one scatterer by rescaling V_B with $\sqrt{M_B}$ times. Around the resonance, the reflection spectrum yields the so-called Breit-Wigner line shape with the spectrum width given by $M_B V_B^2/|J\sin(k_0)|$, where k_0 is determined by the relation $4J^2\sin^2(k)(\omega_k - \Omega_B)^2 = M_B^2 V_B^4$ [5]. In particular, if the photon energy ω_k is under resonance with the two-level scatterers, namely, $\omega_k = \Omega_B$, one then obtains complete reflection with $r_k = -1$ (hence the above-mentioned π phase shift). Under the parameter setting $\omega_c = \Omega_B$, the

resonance scattering condition $\omega_k = \omega_c + 2J\cos(k) = \Omega_B$ occurs for $k = \pi/2$. From the expression of r_k, it is also seen that if $k = 0$ or $k = \pi$, complete reflection happens also. However, this is irrelevant to our self-interference mechanism because such components have a vanishing group velocity in the waveguide. In Fig. 3(b), we show the reflection and transmission spectra versus momentum k.

Cases with two or more emitters.—We now examine how collective emission rates with two QEs can be manipulated by exploiting self-interference. The two emitters are prepared in typical single-photon entangled states $|\psi^{\pm}\rangle = (1/\sqrt{2})(\sigma^{+}_{j_1,A} \pm \sigma^{+}_{j_2,A})|g, \mathrm{vac}\rangle$. For $|\psi^{-}\rangle$, the decay of QEs is completely suppressed since it is a dark state that cannot emit a photon. Thus we focus on the emission dynamics emanating from $|\psi^{+}\rangle$. When $V_B = 0$ and the frequencies of QEs lie outside the scattering band with $|\Delta_A \pm 2J| \gg V_A$, the evolution of $|\psi^{+}\rangle$ is dominated by a trapping regime due to the presence of bound states [56]. For the case $V_A \ll 2J$, the decay of the amplitudes $C^A_{j_1}(t) = C^A_{j_2}(t) \equiv C_2(t)$ is basically exponential, with a very slowly changing radiation rate as Ω_A is tuned from $\omega_c \pm J$ to ω_c. This is what one expects from the Wigner-Weisskopf and Markovian perturbative theories, which predict $|C_2(t)|^2 \approx (1/2)e^{-\Gamma_s(\Delta_A)t}$, with a decay rate $\Gamma_s(\Delta_A) = 4\pi V_A^2 D(\Delta_A)$, where $D(\Delta_A)$ is the density of states for the photon Hamiltonian H_{ph}. $D(\Delta_A)$ reaches its extremum under the resonance condition $\Delta_A = 0$ and $\Gamma_s(0) \equiv \Gamma_s = 2V_A^2/J$, which is twice the normal decay rate shown in Fig. 2. Indeed, this is what the standard superradiance theory predicts.

Consider now what happens if the excitation frequency Ω_A of QEs is around the middle of the band with $|\Delta_A| \ll 2J$ in the presence of scatterers. The frequency Ω_B of the scatterers controls the position of transmission valley of the radiated photon while M_B and V_B determine the valley width. Like the case of one QE, before t reaches t_0, $|C_2(t)|^2$ behaves as a superradiant state without sensing the scatterers. Beyond t_0, the superradiance rate is found to be much enhanced if $\Delta x = 2n + 1$ and much suppressed if $\Delta x = 2n$. Representative results are shown in Fig. 3(c). It is seen that the self-interference mechanism works effectively in the case of superradiance. In particular, the enhanced superradiance by constructive self-interference may be termed hyperradiance, a terminology also used previously but due to different physics [71]. Under the conditions $V_A \ll 2J$ and $\sqrt{M_B}V_B \sim 2J$, we can make reasonable approximations using our general theoretical expressions and find the following hyperradiance dynamics with small Δx [58]:

$$C_2(t) \approx \frac{M_B V_B^2 - J\Gamma_h}{\sqrt{2(\chi^2 - 16 M_B V_A^2 V_B^2)}} e^{-(\Gamma_h/2)t}. \tag{5}$$

Here the radiance rate $\Gamma_h = 4JV_A^2/(J^2 - \Delta x V_A^2)$ with $\chi = M_B V_B^2 - \Delta x M_B V_A^2 V_B^2/J^2$. The dotted line shown in Fig. 3(c) is obtained from Eq. (5), in excellent agreement with exact results obtained directly from Eq. (4). Under the limit Δx being small enough, Γ_h is found to be just 2 times the superradiance rate $\Gamma_h = 2\Gamma_s$. On the other hand, Eq. (5) indicates that Γ_h becomes large as Δx increases. As such, tuning Δx allows us to further boost hyperradiance rates.

Finally, we investigate how the self-interference mechanism works when there are multiple QEs. In this case, we rely fully on computational studies since it becomes tedious to find analytical results with more than two QEs being initially excited. To investigate if the above hyperradiance dynamics can be extended to cases with multiple QEs, we consider the following initial amplitudes: $C^A_{j_1}(0) = \cdots = C^A_{j_{M_A}}(0) = 1/\sqrt{M_A}$. Figure 3(d) depicts the results with $M_A = 5$ QEs for different values of Δx. In the absence of scatterers, under the condition $\sqrt{M_A}V_A \ll 2J$, the amplitudes $C^A_{j_1}(t) = \cdots = C^A_{j_{M_A}}(t) \equiv C_{M_A}(t)$ can be approximately described by $|C_{M_A}(t)|^2 \approx (1/M_A)e^{-\Gamma_s t}$ with $\Gamma_s = M_A V_A^2/J$, which is nothing but the Dicke superradiance.

However, for cases with $\Delta x = 2n + 1$, Fig. 3(d) shows that the self-interference mechanism further boosts the collective emission rates by a factor of 2 for relatively small Δx. Furthermore, as Δx increases, the emission rate continues to be enhanced and hence surpasses $2\Gamma_s$. This echoes with our observation in the case of two emitters. To understand this intriguing trend due to increasing Δx, we first note that the wave vectors of the photon that will be backward scattered are spread around $k = \pi/2$ (in the direction toward the scatterers), but only the component with precisely $k = \pi/2$ of the largest group velocity can optimally induce the constructive self-interference. If Δx increases, the potential phase dispersion among these components along the propagation pathway increases. This imposes a more strict selection on the wave components that can contribute to the self-interference. These selected wave components also tend to induce the self-interference more synchronously.

For cases with $\Delta x = 2n$, it is clearly observed in Fig. 3(d) that the emission rates are much suppressed due to the destructive self-interference. For suppressed subradiance, the asymptotic values of the excited state population is finite at sufficiently long time. Indeed, under $\Delta_B = 0$, the emitted photon is first bounced back by the scatterers. Once the scattered photon meets the QEs, destructive self-interference suppresses the collective emission and as such the QEs tend to reflect the emitted photon as well, thus also dynamically trapping the photon between the QEs and the scatterers. These results and insights indicate the role of bound states in fully explaining the population trapping on the excited state.

Discussion and conclusions.—In a one-dimensional nonlinear waveguide setting, we have shown that the self-interference incurred by a backward scattered photon

originally emitted from quantum emitters can dramatically change the emission rate. This self-interference mechanism then leads to extensive control of the collective emission dynamics, ranging from hyperradiance to strongly suppressed subradiance. The theory and the physics communicated in this Letter are rather general. Indeed, the considered quantum emitters can be of different types, including both natural and artificial ones.

It might not be straightforward to tune the separation between the emitters and the scatterers if they are already grown in a nanophotonic structure. We propose to install several different groups of quantum scatterers at different positions in the waveguide. When the transition frequencies of the scatterers are tuned to be outside the band and far away from the resonance frequency of a single cavity, this group of scatterers can be considered to be turned off and hence irrelevant to our self-interference mechanism. For this reason, one can effectively realize the position tuning of the scatterers by adjusting their resonance frequencies.

The use of coupled superconducting resonators with transmon qubits is a promising route for experimental realization of this Letter [58]. By tuning the external magnetic flux intersecting the loop formed by the SQUID [62], the frequencies of transmon qubits can be tuned in the range of 1 to 10 GHz [1,63]. The high-quality superconducting resonators have frequencies between 5 and 15 GHz [64], thus making the resonator-qubit resonance condition possible. Various chains of coupled superconducting resonators have also been realized and the coupling strength $J/(2\pi)$ has the range from 20 to 730 MHz [65–70]. The qubit-resonator coupling strength is in the range of $V_A/(2\pi), V_B/(2\pi) = 5$–$300$ MHz [2,63], sufficient to yield the range of $V_A/(2J)$ and $V_B/(2J)$ considered in this Letter. Clearly then, the self-interference mechanism uncovered here is within reach of existing experimental capabilities.

J. G. acknowledges fund support by the Singapore Ministry of Education Academic Research Fund Tier-3 Grant No. MOE2017-T3-1-001 (WBS No. A-0004197-00-00).

*qiaolei@nus.edu.sg
†phygj@nus.edu.sg

[1] X. Gu, A. F. Kockum, A. Miranowicz, Y. X. Liu, and F. Nori, Microwave photonics with superconducting quantum circuits, Phys. Rep. **718–719**, 1 (2017).
[2] G. Wendin, Quantum information processing with superconducting circuits: A review, Rep. Prog. Phys. **80**, 106001 (2017).
[3] D. Roy, C. M. Wilson, and O. Firstenberg, Strongly interacting photons in one-dimensional continuum, Rev. Mod. Phys. **89**, 021001 (2017).
[4] J.-T. Shen and S. Fan, Coherent Single Photon Transport in a One-Dimensional Waveguide Coupled with Superconducting Quantum Bits, Phys. Rev. Lett. **95**, 213001 (2005).
[5] L. Zhou, Z. R. Gong, Y. X. Liu, C. P. Sun, and F. Nori, Controllable Scattering of a Single Photon inside a One-Dimensional Resonator Waveguide, Phys. Rev. Lett. **101**, 100501 (2008).
[6] D. E. Chang, A. S. Sorensen, E. A. Demler, and M. D. Lukin, A single-photon transistor using nanoscale surface plasmons, Nat. Phys. **3**, 807 (2007).
[7] M. Rycenga, C. M. Cobley, J. Zeng, W. Li, C. H. Moran, Q. Zhang, D. Qin, and Y. Xia, Controlling the synthesis and assembly of silver nanostructures for plasmonic applications, Chem. Rev. **111**, 3669 (2011).
[8] J. Claudon, J. Bleuse, N. S. Malik, M. Bazin, P. Jaffrennou, N. Gregersen, C. Sauvan, P. Lalanne, and J.-M. Gerard, A highly efficient single-photon source based on a quantum dot in a photonic nanowire, Nat. Photonics **4**, 174 (2010).
[9] P. Lodahl, S. Mahmoodian, and S. Stobbe, Interfacing single photons and single quantum dots with photonic nanostructures, Rev. Mod. Phys. **87**, 347 (2015).
[10] O. Astafiev, A. M. Zagoskin, A. A. Abdumalikov, Jr., Y. A. Pashkin, T. Yamamoto, K. Inomata, Y. Nakamura, and J. S. Tsai, Resonance fluorescence of a single artificial atom, Science **327**, 840 (2010).
[11] J. You and F. Nori, Atomic physics and quantum optics using superconducting circuits, Nature (London) **474**, 589 (2011).
[12] A. A. Houck, H. E. Tureci, and J. Koch, On-chip quantum simulation with superconducting circuits, Nat. Phys. **8**, 292 (2012).
[13] H. Zheng and H. U. Baranger, Persistent Quantum Beats and Long-Distance Entanglement from Waveguide-Mediated Interactions, Phys. Rev. Lett. **110**, 113601 (2013).
[14] G. Z. Song, J. L. Guo, W. Nie, L. C. Kwek, and G. L. Long, Optical properties of a waveguide-mediated chain of randomly positioned atoms, Opt. Express **29**, 1903 (2021).
[15] Z. H. Wang, T. Jaako, P. Kirton, and P. Rabl, Supercorrelated Radiance in Nonlinear Photonic Waveguides, Phys. Rev. Lett. **124**, 213601 (2020).
[16] E. Sánchez-Burillo, L. Martín-Moreno, J. J. García-Ripoll, and D. Zueco, Single Photons by Quenching the Vacuum, Phys. Rev. Lett. **123**, 013601 (2019).
[17] L. Guo, A. F. Kockum, F. Marquardt, and G. Johansson, Oscillating bound states for a giant atom, Phys. Rev. Research **2**, 043014 (2020).
[18] G. Andersson, B. Suri, L. Guo, T. Aref, and P. Delsing, Non-exponential decay of a giant artificial atom, Nat. Phys. **15**, 1123 (2019).
[19] H. Pichler and P. Zoller, Photonic Circuits with Time Delays and Quantum Feedback, Phys. Rev. Lett. **116**, 093601 (2016).
[20] P. Facchi, S. Pascazio, F. V. Pepe, and D. Pomarico, Correlated photon emission by two excited atoms in a waveguide, Phys. Rev. A **98**, 063823 (2018).
[21] A. González-Tudela and J. I. Cirac, Quantum Emitters in Two-Dimensional Structured Reservoirs in the Nonperturbative Regime, Phys. Rev. Lett. **119**, 143602 (2017).
[22] S. Garmon, K. Noba, G. Ordonez, and D. Segal, Non-Markovian dynamics revealed at a bound state in the continuum, Phys. Rev. A **99**, 010102(R) (2019).

[23] G. Calajó, Y.-L. L. Fang, H. U. Baranger, and F. Ciccarello, Exciting a Bound State in the Continuum through Multiphoton Scattering Plus Delayed Quantum Feedback, Phys. Rev. Lett. **122**, 073601 (2019).
[24] F. Dinc and A. M. Brańczyk, Non-Markovian super-superradiance in a linear chain of up to 100 qubits, Phys. Rev. Research **1**, 032042(R) (2019).
[25] E. Sánchez-Burillo, D. Zueco, L. Martín-Moreno, and J. J. García-Ripoll, Dynamical signatures of bound states in waveguide QED, Phys. Rev. A **96**, 023831 (2017).
[26] L. Qiao and C. P. Sun, Atom-photon bound states and non-Markovian cooperative dynamics in coupled-resonator waveguides, Phys. Rev. A **100**, 063806 (2019).
[27] L. Qiao and C. P. Sun, Universal trapping law induced by an atomic cloud in single-photon cooperative dynamics, Phys. Rev. A **101**, 063831 (2020).
[28] R. H. Dicke, Coherence in spontaneous radiation processes, Phys. Rev. **93**, 99 (1954).
[29] M. Gross and S. Haroche, Superradiance: An essay on the theory of collective spontaneous emission, Phys. Rep. **93**, 301 (1982).
[30] K. Sinha, P. Meystre, E. A. Goldschmidt, F. K. Fatemi, S. L. Rolston, and P. Solano, Non-Markovian Collective Emission from Macroscopically Separated Emitters, Phys. Rev. Lett. **124**, 043603 (2020).
[31] A. A. Svidzinsky, J. T. Chang, and M. O. Scully, Dynamical Evolution of Correlated Spontaneous Emission of a Single Photon from a Uniformly Excited Cloud of N Atoms, Phys. Rev. Lett. **100**, 160504 (2008).
[32] G. Y. Slepyan and A. Boag, Quantum Nonreciprocity of Nanoscale Antenna Arrays in Timed Dicke States, Phys. Rev. Lett. **111**, 023602 (2013).
[33] S. D. Jenkins, J. Ruostekoski, N. Papasimakis, S. Savo, and N. I. Zheludev, Many-Body Subradiant Excitations in Metamaterial Arrays: Experiment and Theory, Phys. Rev. Lett. **119**, 053901 (2017).
[34] Y. Ke, A. V. Poshakinskiy, C. Lee, Y. S. Kivshar, and A. N. Poddubny, Inelastic Scattering of Photon Pairs in Qubit Arrays with Subradiant States, Phys. Rev. Lett. **123**, 253601 (2019).
[35] Y.-X. Zhang and K. Molmer, Theory of Subradiant States of a One-Dimensional Two-Level Atom Chain, Phys. Rev. Lett. **122**, 203605 (2019).
[36] T. Bienaimé, N. Piovella, and R. Kaiser, Controlled Dicke Subradiance from a Large Cloud of Two-Level Systems, Phys. Rev. Lett. **108**, 123602 (2012).
[37] D. Plankensteiner, C. Sommer, H. Ritsch, and C. Genes, Cavity Antiresonance Spectroscopy of Dipole Coupled Subradiant Arrays, Phys. Rev. Lett. **119**, 093601 (2017).
[38] M. R. Bakhtiari, A. Hemmerich, H. Ritsch, and M. Thorwart, Nonequilibrium Phase Transition of Interacting Bosons in an Intra-Cavity Optical Lattice, Phys. Rev. Lett. **114**, 123601 (2015).
[39] K. Yamamoto, M. Nakagawa, N. Tsuji, M. Ueda, and N. Kawakami, Collective Excitations and Nonequilibrium Phase Transition in Dissipative Fermionic Superfluids, Phys. Rev. Lett. **127**, 055301 (2021).
[40] N. Skribanowitz, I. P. Herman, J. C. MacGillivray, and M. S. Feld, Observation of Dicke Superradiance in Optically Pumped HF Gas, Phys. Rev. Lett. **30**, 309 (1973).
[41] M. Gross, C. Fabre, P. Pillet, and S. Haroche, Observation of Near-Infrared Dicke Superradiance on Cascading Transitions in Atomic Sodium, Phys. Rev. Lett. **36**, 1035 (1976).
[42] S. Inouye, A. Chikkatur, D. Stamper-Kurn, J. Stenger, D. Pritchard, and W. Ketterle, Superradiant Rayleigh scattering from a Bose-Einstein condensate, Science **285**, 571 (1999).
[43] K. Baumann, C. Guerlin, F. Brennecke, and T. Esslinger, Dicke quantum phase transition with a superfluid gas in an optical cavity, Nature (London) **464**, 1301 (2010).
[44] R. G. DeVoe and R. G. Brewer, Observation of Superradiant and Subradiant Spontaneous Emission of Two Trapped Ions, Phys. Rev. Lett. **76**, 2049 (1996).
[45] S. Begley, M. Vogt, G. K. Gulati, H. Takahashi, and M. Keller, Optimized Multi-Ion Cavity Coupling, Phys. Rev. Lett. **116**, 223001 (2016).
[46] B. Casabone, K. Friebe, B. Brandstatter, K. Schuppert, R. Blatt, and T. E. Northup, Enhanced Quantum Interface with Collective Ion-Cavity Coupling, Phys. Rev. Lett. **114**, 023602 (2015).
[47] J. A. Mlynek, A. A. Abdumalikov, C. Eichler, and A. Wallraff, Observation of Dicke superradiance for two artificial atoms in a cavity with high decay rate, Nat. Commun. **5**, 5186 (2014).
[48] S. Filipp, A. F. van Loo, M. Baur, L. Steffen, and A. Wallraff, Preparation of subradiant states using local qubit control in circuit QED, Phys. Rev. A **84**, 061805(R) (2011).
[49] Z. Wang, H. Li, W. Feng, X. Song, C. Song, W. Liu, Q. Guo, X. Zhang, H. Dong, D. Zheng, H. Wang, and D.-W. Wang, Controllable Switching between Superradiant and Subradiant States in a 10-Qubit Superconducting Circuit, Phys. Rev. Lett. **124**, 013601 (2020).
[50] M. S. Mendes, P. L. Saldanha, J. W. R. Tabosa, and D. Felinto, Dynamics of the reading process of a quantum memory, New J. Phys. **15**, 075030 (2013).
[51] M. O. Scully, Single Photon Subradiance: Quantum Control of Spontaneous Emission and Ultrafast Readout, Phys. Rev. Lett. **115**, 243602 (2015).
[52] M. Woldeyohannes and S. John, Coherent control of spontaneous emission near a photonic band edge: A qubit for quantum computation, Phys. Rev. A **60**, 5046 (1999).
[53] M. Woldeyohannes and S. John, Coherent control of spontaneous emission near a photonic band edge, J. Opt. B **5**, R43 (2003).
[54] X. Q. Jiang, B. Zhang, Z. W. Lu, and X. D. Sun, Control of spontaneous emission from a microwave-field-coupled three-level Λ-type atom in photonic crystals, Phys. Rev. A **83**, 053823 (2011).
[55] F. Lombardo, F. Ciccarello, and G. M. Palma, Photon localization versus population trapping in a coupled-cavity array, Phys. Rev. A **89**, 053826 (2014).
[56] S. John and T. Quang, Spontaneous emission near the edge of a photonic band gap, Phys. Rev. A **50**, 1764 (1994).
[57] L. Qiao, Y. J. Song, and C. P. Sun, Quantum phase transition and interference trapping of populations in a coupled-resonator waveguide, Phys. Rev. A **100**, 013825 (2019).
[58] See Supplemental Material at http://link.aps.org/supplemental/10.1103/PhysRevLett.129.093602, which includes Refs. [1,2,5,56,57,59–70], for further details on our

theoretical treatments and a promising route for experimental realization.

[59] E. N. Economou, *Green Functions in Quantum Physics* (Springer-Verlag, Berlin, 1979).

[60] N. Meher and S. Sivakumar, Quantum information processing in cavities: A review, arXiv:2204.01322.

[61] A. Wallraff, D. I. Schuster, A. Blais, L. Frunzio, R. H. J. Majer, S. Kumar, S. M. Girvin, and R. J. Schoelkopf, Strong coupling of a single photon to a superconducting qubit using circuit quantum electrodynamics, Nature (London) **431**, 162 (2004).

[62] J. Koch, T. M. Yu, J. Gambetta, A. A. Houck, D. I. Schuster, J. Majer, A. Blais, M. H. Devoret, S. M. Girvin, and R. J. Schoelkopf, Charge-insensitive qubit design derived from the Cooper pair box, Phys. Rev. A **76**, 042319 (2007).

[63] A. Blais, A. L. Grimsmo, S. M. Girvin, and A. Wallraff, Circuit quantum electrodynamics, Rev. Mod. Phys. **93**, 025005 (2021).

[64] A. Blais, S. M. Girvin, and W. D. Oliver, Quantum information processing and quantum optics with circuit quantum electrodynamics, Nat. Phys. **16**, 247 (2020).

[65] N. M. Sundaresan, R. Lundgren, G. Zhu, A. V. Gorshkov, and A. A. Houck, Interacting Qubit-Photon Bound States with Superconducting Circuits, Phys. Rev. X **9**, 011021 (2019).

[66] V. S. Ferreira, J. Banker, A. Sipahigil, M. H. Matheny, A. J. Keller, E. Kim, M. Mirhosseini, and O. Painter, Collapse and Revival of an Artificial Atom Coupled to a Structured Photonic Reservoir, Phys. Rev. X **11**, 041043 (2021).

[67] M. Fitzpatrick, N. M. Sundaresan, A. C. Y. Li, J. Koch, and A. A. Houck, Observation of a Dissipative Phase Transition in a One-Dimensional Circuit QED Lattice, Phys. Rev. X **7**, 011016 (2017).

[68] D. C. McKay, R. Naik, P. Reinhold, L. S. Bishop, and D. I. Schuster, High-Contrast Qubit Interactions Using Multimode Cavity QED, Phys. Rev. Lett. **114**, 080501 (2015).

[69] M. Scigliuzzo, G. Calajò, F. Ciccarello, D. P. Lozano, A. Bengtsson, P. Scarlino, A. Wallraff, D. Chang, P. Delsing, and S. Gasparinetti, Extensible Quantum Simulation Architecture Based on Atom-Photon Bound States in an Array of High-Impedance Resonators, arXiv:2107.06852 [Phys. Rev. X (to be published)].

[70] E. Kim, X. Zhang, V. S. Ferreira, J. Banker, J. K. Iverson, A. Sipahigil, M. Bello, A. González-Tudela, M. Mirhosseini, and O. Painter, Quantum Electrodynamics in a Topological Waveguide, Phys. Rev. X **11**, 011015 (2021).

[71] M.-O. Pleinert, J. von Zanthier, and G. S. Agarwal, Hyperradiance from collective behavior of coherently driven atoms, Optica **4**, 779 (2017).